OPTICAL CERENKOV MEASUREMENTS OF EMITTANCE GROWTH IN THE ADVANCED TEST ACCELERATOR BEAM UNDER LASER ION-GUIDING

Y.P. Chong, F.J. Deadrick, D.G. Hirzel, J.S. Kallman, P. Lee, J.F. Poulter, W.E. Rivera, P.L. Stephan, and J.T. Weir

Lawrence Livermore National Laboratory
P.O. Box 808, L-626
Livermore, CA 94550

Abstract

A new beam profile diagnostic using optical Cerenkov radiation from a quartz foil has been deployed at the Advanced Test Accelerator (ATA) at Lawrence Livermore National Laboratory. Quartz has been found to perform better than previously tested foils (titanium and Kapton) in terms of damage threshold. The emission intensity from quartz is over an order of magnitude brighter than that from graphite foil. Data were taken at the beginning, middle, and end of ATA, i.e., at 3.8 MeV (cell 15), 22.5 MeV (cell 90), and 43 MeV (11 m beyond the end). Profile measurements of the ion-focused beam showed emittance growth through the pulse. Double-Gaussian fits to the radial profile were often superior to single-Gaussian fits and showed that a large beam dominated the second half of the pulse. This was observed for currents of 1, 3, and 7 kA at the accelerator output and at cell 15 for the 3-kA case. The dependence of emittance growth on several parameters was studied.

Introduction

Transport of the ATA beam under laser ion guiding has been studied during the past year in order to gain insight into the source of emittance degradation in the output pulse. This paper describes the beam profile diagnostic and measurements made using gated 2-D image-intensified CCD TV cameras to detect optical Cerenkov radiation emitted by the e-beam striking quartz foils.

Beam profiles of the ATA beam have been measured primarily by detecting x-ray or optical emissions from targets inserted into the beam path. Target materials tested so far have suffered from marginal survivability. For optical emissions, understanding the process that generates the radiation has been difficult in the case of titanium and graphite. Although graphite survives well, the emission intensity is low and appears to have a threshold. Thin (0.038-cm) quartz foils have been found to withstand damage at beam current densities up to 55 kA/cm^2. The survivability of quartz foils with a well-understood radiation source has alleviated these difficulties.

Cerenkov Radiation

Promptness

Temporal behavior of the emission was compared to that of an adjacent wall-current monitor. The emission intensity was integrated over the foil surface by imaging onto the 18-mm-diam photocathode of a photometer (Hamamatsu R1194U). The peak optical signal was normalized to the peak of the beam-bug current. Figure 1 shows that the optical signal follows the beam current closely on both rise and fall edges. The ringing observed at the peak and tail of the optical signal was caused by a mismatch in the photometer output impedance.

Angular Dependence of Emission

As shown in Fig. 2, Cerenkov radiation from the rear surface of a thin quartz foil was detected with a gated 2-D image-intensified TV camera. Calculations for the peak emission angle predicted that at a foil angle of 83° to the beamline, the Cerenkov axis was aligned to the optical line of sight (LOS). An intensity sharply peaked at this angle was indeed observed using a foil with clear smooth surfaces. The emission was so intense that it saturated the camera at zero gain. In contrast, the MCP gain on the camera was often set at maximum for graphite or titanium foil emissions. This indicates that Cerenkov emission from quartz is at least 15 times brighter. Tilting the foil 8° on either side of the peak angle resulted in an intensity drop of two orders of magnitude. This angular dependence confirmed that the emission detected was Cerenkov radiation. For ease of interpretation during operations, the foil was typically set at 45° and the rear surface was diffused. At high beam current density, neutral density filters were inserted to prevent camera saturation.

Data Reduction

The bright Cerenkov source permitted finer temporal resolution and wider dynamic range than was possible for emissions from previous materials deployed. Gate widths were narrowed down to 5 ns in the 2-D TV cameras. In contrast, gate widths were seldom below 10 ns for graphite or titanium foils. Data frames were acquired and digitized as the gate was walked through the pulse. Profiles in the x and y directions through the image were initially fit to single-Gaussian curves. The amplitude, position, width, and background were varied. It was found that these fits were not acceptable in most cases. Instead, a double-Gaussian fit was required and it reduced χ^2 by a factor of 10 to 20 (Fig. 3). An

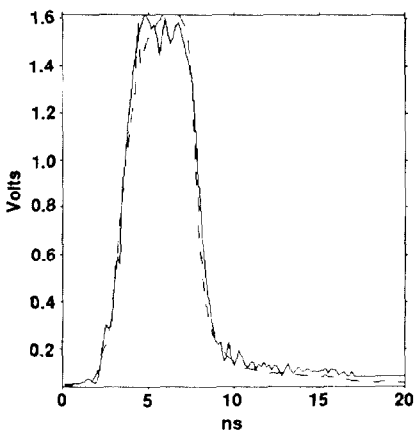

Figure 1. Photometer signal shows spatially-integrated intensity is prompt compared to neighboring current monitor.

*Performed jointly under the auspices of the U.S. DOE by LLNL under W-7405-ENG-48 and for the DOD under DARPA, ARPA Order No. 4395, monitored by NSWC.

CH2669-0/89/0000-1495$01.00©1989 IEEE

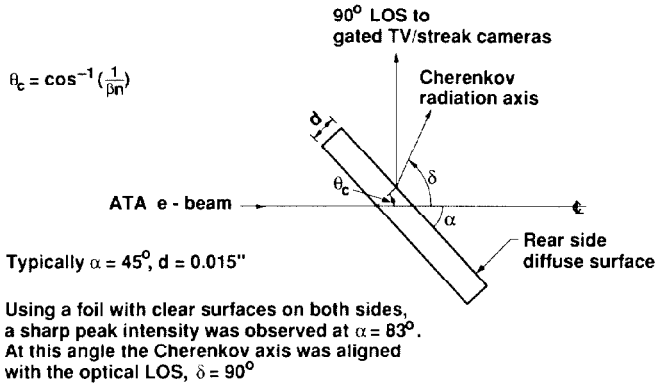

Figure 2. Cerenkov foil optical diagnostic.

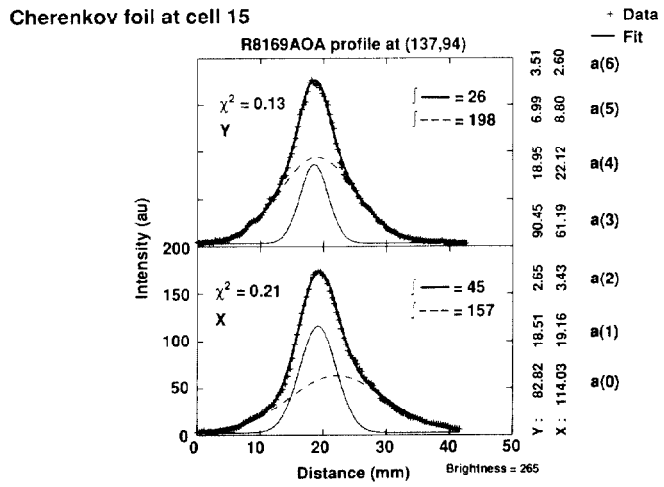

Figure 3. Typical example of a two-component beam at cell 15.

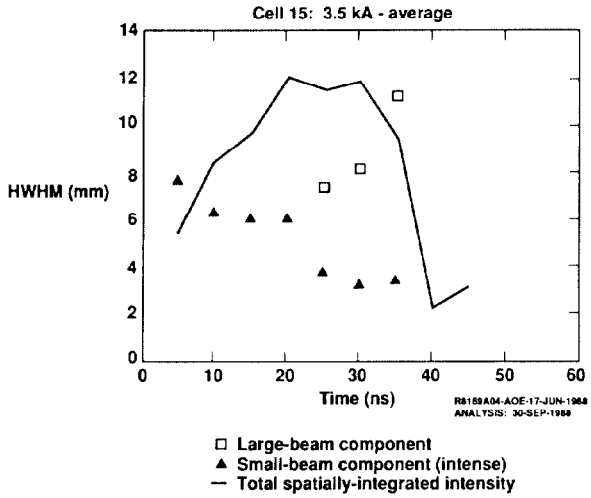

Figure 4. Cerenkov foil shows presence of two-component beam at cell 15.

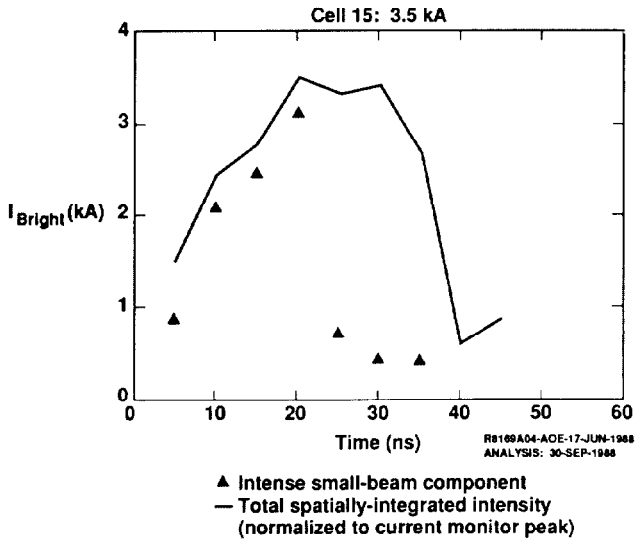

Figure 5. Current profile of intense small-beam component from double-Gaussian beam at cell 15.

example at cell 15 (Fig. 4) shows that the beam consists of two components: a small, intense beam of 1 cm at the head narrowing to 0.7 cm after 20 ns, and a second beam 2-5 times bigger. The total intensity is shown (assuming axisymmetry) where the peak intensity has been normalized to the peak beam current. From the fit, the amount of current carried by each component was obtained (Fig. 5). The first half of the pulse was in the small component, rising to 3 kA. The second half was carried in the large component so that, overall, the beam was seen to grow rapidly after 20 ns.

Results

Current and Accelerator Length Dependence

In Fig. 6, an overview of the beam profiles for I = 1, 3, 7 kA is shown as a function of accelerator length. At cell 15, the beam has been accelerated through a 5-cell block after being matched at the collimator. At cell 90, the beam is tightly pinched on the ion channel, resulting in minimum radii from 0.3 to 0.15 cm. At the 11-m LOS, the beam has been taken off ion guiding and transported under quadrupole control. Two beam components are clearly observed.

It is clear that significant emittance growth was already present at cell 15 for the high current case. This may be attributed to 1) the injector beam, 2) matching onto the channel, 3) the collimator, or 4) ion motion. There is a definite scaling with current level. Even at cell 15, the rate at which emittance degrades with current is obvious.

Pressure Dependence

The dependence of emittance growth on benzene pressure is not strong. Neither doubling the collimator pressure to 0.2 μm nor reducing it to 0.05 μm produced a change at cell 15. Nominal pressures during operation were 0.1 μm in the collimator and 0.2 μm in the accelerator.

Comparison of Bow Probe and Optical Data

Bow probes were installed at cells 15 and 90, so comparison is possible only at these locations. At cell 90, fits of single-Gaussian profiles to probe

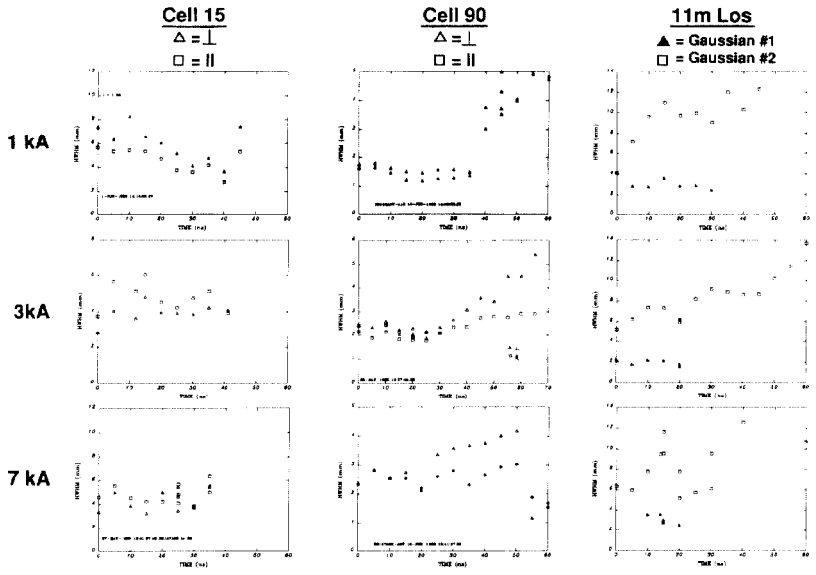

Figure 6. Cerenkov foil data for different currents at different accelerator locations.

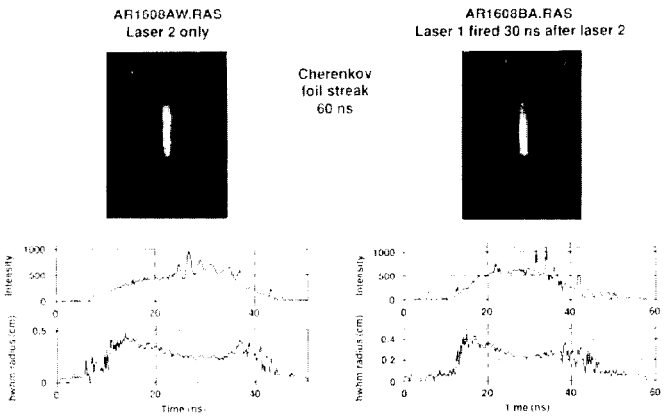

Figure 7. Extending laser pulse width by firing a second laser shows no significant improvement in emittance growth.

data were sufficient except in the low current case. However, optical data fits at cell 90 needed only single Gaussians at all currents. At cell 15, optical data were not available for comparison for the low and high currents. This was due to an inadvertently high setting for the camera threshold. After the setting was adjusted, the 3-kA case showed good agreement between probe and optical data results. It was concluded that the optical and bow probe diagnostics agreed in almost all cases.

Laser Pulse Length

An experiment was done to see the effect of lengthening the guide laser pulse with a second collinear laser. The first laser was set at the usual timing relative to the accelerator. The second laser was fired at various delays (-30, 0, 50, 100 ns) relative to the first laser. No significant change in emittance growth was observed according to the streak camera view of the Cerenkov foil (Fig. 7).

Summary

The Cerenkov foil diagnostic performed extremely well, producing very high levels of optical emission. At the angle yielding peak intensity, the camera was saturated at zero gain setting. Such a bright source allowed productive operation of the streak camera which had hitherto been hindered by low light levels from other foil emission processes. The survivability of quartz foils up to 55 kA/cm^2 has enabled beam profile measurements inside the ion channel. This had not been achieved previously. Detailed time behavior of beam profiles was obtained for three current levels--1, 3, and 7 kA--and at the beginning, middle, and end of the accelerator. Emittance growth through the pulse was observed to scale with current and to be insensitive to laser pulse length and benzene pressure in the collimator. At high current, emittance degradation was already significant at the front end of the accelerator, indicating possible causes in the injector or collimator or matching on the channel, or ion motion. Double-Gaussian beam profiles were often observed with the larger beam dominating the latter half of the pulse. In general, probe and optical data agreed.

Acknowledgments

We gratefully thank Charlie Frost and Ed Paterson of Sandia National Laboratory for first recommending thin quartz as a Cerenkov foil diagnostic. We also sincerely thank the ATA operations crew for their intensive and enthusiastic efforts.